JOURNAL OF MOLECULAR SPECTROSCOPY **159**, 534–550 (1993)

High-Resolution Fourier Transform Infrared Spectrum of the ν_5 Fundamental Band System of Cyanogen, NCCN

JOHN C. GRECU, BRENDA P. WINNEWISSER, AND MANFRED WINNEWISSER

Physikalisch-Chemisches Institut der Justus-Liebig Universität, Heinrich-Buff-Ring 58, W-6300 Giessen, Germany

The far-infrared spectrum of the lowest-lying rovibrational band system ν_5 of cyanogen, NCCN, was measured in the wavenumber range from 180 to 280 cm^{-1}. A Fourier transform spectrometer was used with a nominal resolution of 0.0018 cm^{-1}. Transitions within the ν_5 manifold up to $v_5 = 4$ were assigned and precise molecular constants for the corresponding states were determined.

INTRODUCTION

Cyanogen,[1] NCCN, was first synthesized by Gay-Lussac in 1815 by thermolysis of AgCN (*1*). The problem of the determination of the chemical formula and structure of cyanogen accompanied chemistry from its early days (*2, 3*). Even now, with investigations by means of high-resolution gas-phase spectroscopy and ab initio calculations at a high level, cyanogen still presents questions about details of its structure and dynamics.

Cyanogen belongs to the point group $D_{\infty h}$ and exhibits five fundamental normal modes, two of which are degenerate. The fundamental rovibrational band systems ν_1 at 2330.5 cm^{-1}, ν_2 at 845.5 cm^{-1}, and ν_4 at 502.8 cm^{-1} are infrared-inactive due to the centrosymmetry of the molecule. The *ungerade* modes ν_3 at 2157.8 cm^{-1} and ν_5 at 233.9 cm^{-1} are infrared-active fundamental band systems.

The most recent work on rovibrational spectroscopy of NCCN was carried out by Wang and Weber on the Raman-active band systems (*4*). The infrared spectrum of the ν_3 band system was recorded by Picard (*5*) and the ν_5 band system was observed by Jolma (*6*). The latter study was made with a resolution of 0.02 cm^{-1}. Due to the lack of a permanent electric dipole moment, pure rotational spectra are observable only as Raman spectra, most recently reported in 1987 (*7*).

In the early 1980's cyanogen won new interest upon its detection in the atmosphere of the Saturn moon Titan by Voyager 1 (*8, 9*) and due to the identification of new isomers (*10, 11*). This resulted in new theoretical investigations of cyanogen and its isotopomers concerning the structure, energy levels, and the intensities of vibrational transitions (*12, 13*).

We decided to measure the ν_5 band system, which was first observed by Rubens and von Wartenberg in 1911 (*14*), with high resolution (0.0018 cm^{-1}) and to characterize the lowest rovibrational energy levels, important for the analysis of all other band systems of cyanogen. Furthermore, we carried out precise intensity measurements, which will be treated in the following paper (*15*).

[1] IUPAC name since 1970: Ethanedinitrile.

0022-2852/93 $5.00

EXPERIMENTAL DETAILS

Synthesis

Cyanogen was prepared in two different ways (*2, 3*). The first method was vapor thermolysis of silver cyanide, AgCN:

$$2AgCN \xrightarrow{\Delta} 2Ag + NCCN.$$

Solid AgCN was held under vacuum in a quartz tube with a cross section of ≈ 1 cm^2 at a temperature of 300°C to dry the probe completely. The quartz tube was heated on a length of $\approx$20 cm. After $\approx$1 hr the temperature was raised to 600°C and the product of the pyrolysis was condensed at liquid nitrogen temperature. The product was used without further purification. The yield is quantitative.

The second preparation uses the oxidation of potassium cyanide, KCN, with copper(II) sulfate, $CuSO_4$:

$$2CuSO_4 + 4KCN \rightarrow 2CuCN + 2K_2SO_4 + NCCN.$$

An aqueous solution of KCN was dropped onto solid $CuSO_4 \cdot 5\ H_2O$ in a dry N_2 atmosphere. The gaseous products were passed through an ice/NaCl-cooled trap, through a tube filled with $CaCl_2$, and finally condensed in a trap held at −80°C. This crude product was additionally passed through a tube filled with solid NaOH to eliminate the by-product HCN. The overall yield is 38%.

No impurities were observed. Pure cyanogen is stable in a glass cell.

Far-Infrared (FIR) Measurements

The FIR spectra were recorded with the Bruker IFS 120 HR Fourier transform vacuum Michelson interferometer (*16, 17*).

The glass cell was 10 cm in diameter and 284 cm in length. Wedged polyethylene windows of about 2-mm thickness were used. Cyanogen was sublimed into the cell at room temperature until a sample pressure of 0.25 mbar was reached. The measurement parameters were as follows: source, mercury lamp; aperture, 4 mm; beam splitter, 6 μ mylar; scanner speed, 2.532 cm/sec; optical filters, 0–375 cm^{-1}; detector, Si bolometer, 4.2 K, resolution [1/(maximum optical path difference)], 0.0018 cm^{-1}.

The cyanogen spectrum was recorded in eight blocks each of 25 scans. Since during the measurements the conditions of the spectrometer and sample were stable, all blocks could be coadded.

The spectrum file was divided by a background recorded at lower resolution and post transform zero-filled to match the resolution of the sample spectrum. The resulting transmittance spectrum was further zero-filled to an overall zero-filling factor of 16. The signal-to-noise (S/N) ratio varies between 80 and 100. The peak positions were determined using the available Bruker software.

Calibration was achieved with internal, pure rotational water lines, due to residual water in the spectrometer (not in the sample!). Since the line density of cyanogen increases very rapidly above 215 cm^{-1} only water lines below 210 cm^{-1} are used for calibration purposes. In Table I the water lines used for calibration are listed together with the standard deviation of the calibration fit. If a linear calibration curve can be assumed, the accuracy of the line positions is $\pm 7 \times 10^{-5}$ cm^{-1} at 180 cm^{-1} and $\pm 10 \times 10^{-5}$ cm^{-1} at 250 cm^{-1}.

TABLE I

Pure Rotational Water Lines Used for Internal Calibration

Measured position/ cm^{-1}	Reference position/ cm^{-1}	Calculated position/ cm^{-1}	Deviation 10^5(calc–ref)/ cm^{-1}
173.281 172	173.282 07	173.282 012 8	-5.724 5
173.354 784	173.355 56	173.355 625 1	6.511 1
178.485 051	178.485 89	178.485 917 0	2.700 5
179.047 923	179.048 74	179.048 791 7	5.173 4
184.564 179	184.565 05	184.565 074 5	2.450 0
184.770 620	184.771 51	184.771 516 5	0.650 3
193.478 370	193.479 32	193.479 308 7	-1.124 7
194.321 321	194.322 24	194.322 263 8	2.384 1
195.804 561	195.805 63	195.805 511 0	-11.895 6
197.085 534	197.086 40	197.086 490 3	9.025 3
197.263 671	197.264 72	197.264 628 1	-9.188 0
Standard error of measurement: 6.55 × 10^{-5} cm^{-1}			

THEORETICAL CONSIDERATIONS

For clarity the notation is briefly explained. We refer to a "state" as a group of energy levels designated by a set of vibrational quantum numbers, in the case of a four atomic linear molecule written as $(v_1v_2v_3v_4v_5)$, whereby leading quantum numbers may be omitted if they are zero. Here we need only (v_4v_5). The ν_5 band system in absorption includes only transitions with $\Delta v_5 = +1$, e.g., transitions of the vibrational bands

$$(v_1v_2v_3v_4(v_5+1)) \leftarrow (v_1v_2v_3v_4v_5).$$

If a state involves one or more excited bending modes it splits into two or more substates characterized by the vibrational angular momenta quantum numbers l_i, e.g., $(v_1v_2v_3v_4^{l_4}v_5^{l_5})^k$ with $k = l_4 + l_5$. The transitions between substates constitute subbands, e.g., for the perpendicular bands studied here

$$(v_1v_2v_3v_4^{l_4'}(v_5+1)^{l_5'})^{k\pm1} \leftarrow (v_1v_2v_3v_4^{l_4''}v_5^{l_5''})^k.$$

The rotational energy levels of a linear molecule within a vibrational state or substate can be expressed in a power series (ps) in $J(J+1)$:

$$E(J) = G_c + B_{ps}J(J+1) + D_{ps}J^2(J+1)^2 + H_{ps}J^3(J+1)^3. \quad (1)$$

G_c is defined by band centers and thus differs from the spectroscopic term value G_v defined below, which defines band origins. The expression in Eq. (1) cannot describe a complete k-polyade of an excited bending state simultaneously. Therefore the power series coefficients provide only a nearly "model-free" representation of the energy levels of a state with an excited bending mode. They provide a check of the quality of the data and a basis for the vibrational assignments, but are not directly related to a molecular Hamiltonian.

For the full analysis of the transitions we used the effective Hamiltonian for a linear molecule defined by Yamada *et al.* (*18*). For states within the ν_5 manifold (bending mode ν_t, $v_t = n$ and $l_t = k$) the diagonal elements in k are

$$E_{k,k} = G_v + x_kk^2 + y_kk^4 + \{B_v + d_{Jk}k^2\}f_0(k) - \{D_v + h_{Jk}k^2\}f_0(k)^2, \quad (2)$$

and the only off-diagonal elements needed to reproduce the date are given by

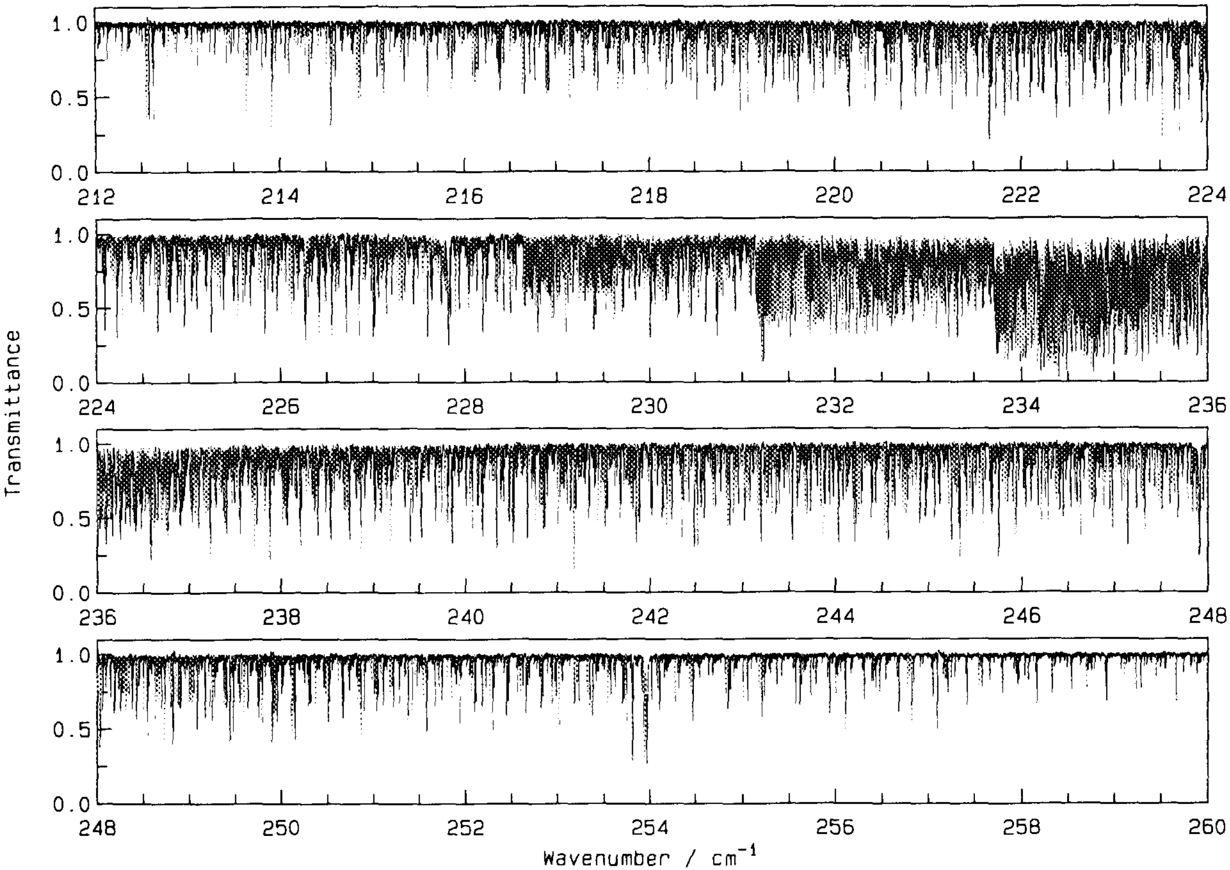

FIG. 1. Overview spectrum of NCCN recorded at 0.25 mbar in a cell 284 cm long at 0.0018 cm^{-1} resolution.

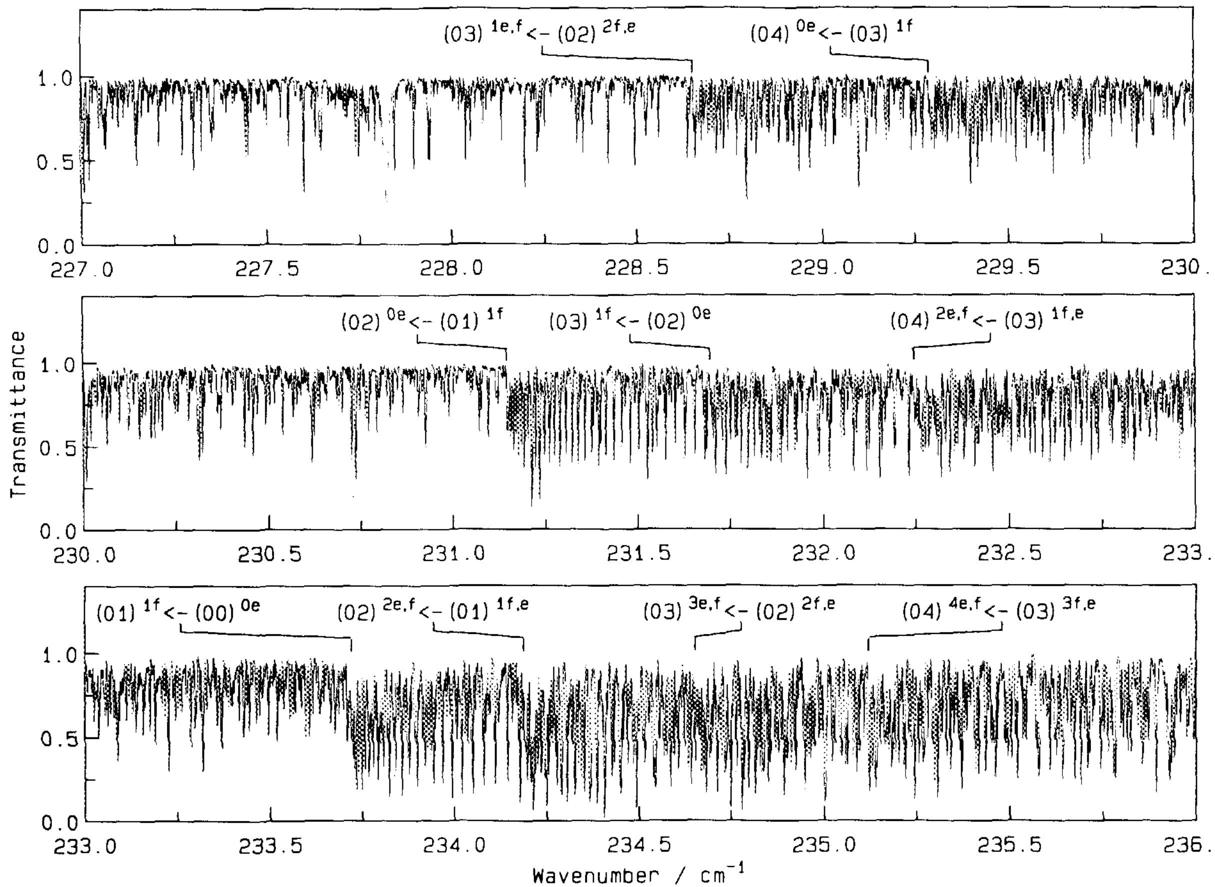

FIG. 2. Q-branch region of the ν_5 band system of NCCN.

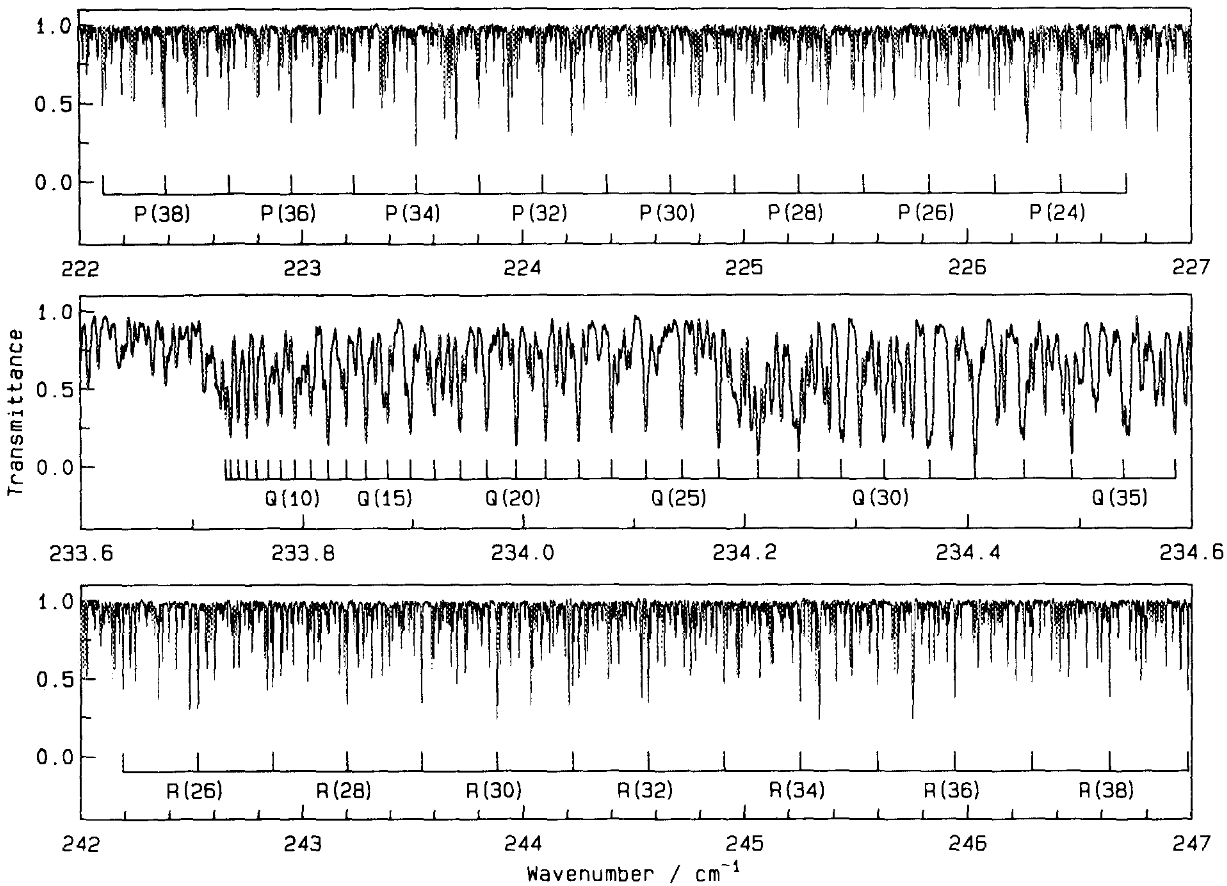

FIG. 3. Excerpts of *P*-, *Q*-, and *R*-branch regions of the ν_5 band system of NCCN. The lines of the fundamental band are indicated with assignment combs.

TABLE II

Band Centers $\nu_c = (G'_c - G''_c)$ Derived from Fits to the Power Series in Eq. (1) of the Subbands in the ν_5 Band System of NCCN. σ is the Standard Deviation of the Fit (the Numbers in Parentheses Give One Standard Deviation in Units of the Last Digits Given)

Subband	$\tilde{\nu}_c/\text{cm}^{-1}$	$10^4\,\sigma/\text{cm}^{-1}$
$(01)^{1e} \leftarrow (00)^{0e}$	233.721 478 (16)	1.01
$(01)^{1f} \leftarrow (00)^{0e}$	233.721 36 (10)	3.56
$(02)^{2e} \leftarrow (01)^{1e}$	234.187 781 (41)	1.76
$(02)^{2f} \leftarrow (01)^{1f}$	234.187 537 (26)	1.31
$(02)^{0e} \leftarrow (00)^{1e}$	231.144 702 (36)	1.69
$(02)^{0e} \leftarrow (01)^{1f}$	231.145 93 (23)	9.58
$(03)^{3e} \leftarrow (02)^{2e}$	234.653 37 (18)	8.01
$(03)^{3f} \leftarrow (02)^{2f}$	234.653 572 (53)	2.50
$(03)^{1e} \leftarrow (02)^{0e}$	231.696 458 (47)	2.16
$(03)^{1f} \leftarrow (02)^{0e}$	231.696 07 (13)	3.69
$(03)^{1e} \leftarrow (02)^{2e}$	228.653 543 (72)	1.76
$(03)^{1f} \leftarrow (02)^{2f}$	228.640 37 (14)	1.70
$(04)^{4e} \leftarrow (03)^{3e}$	235.119 681 (68)	2.28
$(04)^{4f} \leftarrow (03)^{3f}$	235.119 484 (44)	1.38
$(04)^{2e} \leftarrow (03)^{1e}$	232.242 26 (25)	4.83
$(04)^{2f} \leftarrow (03)^{1f}$	232.243 42 (15)	4.01
$(04)^{0e} \leftarrow (03)^{1e}$	229.287 51 (13)	3.75
$(04)^{0e} \leftarrow (03)^{1f}$	229.287 94 (38)	6.12

$$U^{S}_{k,k+2} = U^{S}_{k-2,k} = \tfrac{1}{4}\{q_t + q_{tJ}J(J+1)\}\sqrt{(n-k+1)(n+k+1)}\,f_2(k). \quad (3)$$

The superscript S indicates that this matrix element is defined for the excitation of only one bending mode. The $f_i(k)$ are given by

$$f_0(k) = J(J+1) - k^2 \text{ and}$$

$$f_2(k) = \sqrt{[J(J+1) - k(k+1)][J(J+1) - (k+1)(k+2)]}. \quad (4)$$

With Eqs. (2) and (3) all substates in k of a bending state v_t can be described with one set of parameters.

TABLE III

Power Series (ps) Rotational Constants Obtained from the FIR Spectrum of NCCN (the Numbers in Parentheses Give One Standard Deviation in Units of the Last Digits Given)

Level	from Subband	B_{ps}/cm^{-1}	$10^8\,D_{ps}/\text{cm}^{-1}$	$10^{13}\,H_{ps}/\text{cm}^{-1}$
$(00)^{0e}$	$(01)^{1e} \leftarrow (00)^{0e}$	0.157 088 07 (19)	2.116 3 (18)	
$(01)^{1e}$	$(01)^{1e} \leftarrow (00)^{0e}$	0.157 515 66 (19)	2.180 3 (18)	
$(01)^{1f}$	$(01)^{1f} \leftarrow (00)^{0e}$	0.157 738 56 (25)	2.243 2 (54)	
$(02)^{2e}$	$(02)^{2e} \leftarrow (01)^{1e}$	0.158 160 54 (58)	5.30 (13)	-6.365 (59)
$(02)^{2f}$	$(02)^{2f} \leftarrow (01)^{1f}$	0.158 161 64 (30)	2.302 9 (37)	
$(02)^{0e}$	$(02)^{0e} \leftarrow (01)^{1e}$	0.158 164 85 (39)	4.074 1 (54)	6.442 (20)
$(03)^{3e}$	$(03)^{3e} \leftarrow (02)^{2e}$	0.158 708 5 (50)	4.28 (35)	1.164 (91)
$(03)^{3f}$	$(03)^{3f} \leftarrow (02)^{2f}$	0.158 689 70 (67)	1.636 (11)	
$(03)^{1e}$	$(03)^{1e} \leftarrow (02)^{0e}$	0.158 469 13 (54)	2.759 1 (76)	
$(03)^{1f}$	$(03)^{1f} \leftarrow (02)^{2f}$	0.158 384 8 (40)	4.25 (28)	
$(04)^{4e}$	$(04)^{4e} \leftarrow (03)^{3e}$	0.159 219 91 (87)	1.983 (19)	
$(04)^{4f}$	$(04)^{4f} \leftarrow (03)^{3f}$	0.159 219 29 (56)	1.993 (14)	
$(04)^{2e}$	$(04)^{2e} \leftarrow (03)^{1e}$	0.159 215 2 (32)	2.91 (15)	
$(04)^{2f}$	$(04)^{2f} \leftarrow (03)^{1f}$	0.159 241 8 (19)	3.62 (12)	8.0 (16)
$(04)^{0e}$	$(04)^{0e} \leftarrow (03)^{1e}$	0.159 224 9 (36)	7.37 (24)	-18.4 (50)

TABLE IV

Spectroscopic Constants of NCCN in the Effective Hamiltonian (the Numbers in Parentheses Give One Standard Deviation in Units of the Last Digits Given)

	Vibrational constants			
State	G_v/cm^{-1}	x_k/cm^{-1}	$10^5\, y_k/\mathrm{cm}^{-1}$	
(00)	0.0			
(01)	233.879 144 (23)[a]			
(02)	464.866 405 (35)	0.918 829 6 (90)		
(03)	695.812 505 (46)	0.908 716 7 (64)		
(04)	925.850 387 (51)	0.897 639 0 (11)	6.687 (68)	
	Rotational constants			
State	B_v/cm^{-1}	$10^3(B_v - B_0)/\mathrm{cm}^{-1}$	$10^7\, d_{Jk}/\mathrm{cm}^{-1}$	
(00)	0.157 087 69 (14)	0.0		
(01)	0.157 626 63 (14)[a]	0.538 94 (20)		
(02)	0.158 163 80 (14)	1.076 11 (20)	-5.29 (13)	
(03)	0.158 698 47 (15)	1.610 78 (21)	-6.74 (10)	
(04)	0.159 230 77 (6)	2.143 08 (15)	-7.67 (5)	
State	$10^8\, D_v/\mathrm{cm}^{-1}$	$10^{11}\, h_{Jk}/\mathrm{cm}^{-1}$	$10^4\, q_5/\mathrm{cm}^{-1}$	$10^{10}\, q_{5J}/\mathrm{cm}^{-1}$
(00)	2.110 6 (16)			
(01)	2.205 1 (17)[a]		2.228 24 (23)	6.114 (80)
(02)	2.299 5 (19)	1.82 (38)	2.232 95 (48)	5.978 (97)
(03)	2.397 8 (29)	2.76 (37)	2.240 88 (31)	6.14 (14)
(04)	2.475 1 (16)	5.00 (17)	2.246 25 (87)	4.10 (34)

[a] For determination of the v_5-dependence of G_v, B_v, and D_v extrapolated values of x_k, d_{Jk}, and h_{Jk} were substracted from these values.

An intensity alternation of spectral transitions arising from the spin statistics of adjacent rotational levels is characteristic for molecules with symmetrically equivalent atoms. The spin statistics for NCCN are derived by considering the symmetry representation (Γ) with respect to the exchange of equivalent atoms. Following the Born–Oppenheimer approximation the total wavefunction describing the state of the molecule can be written as

$$\Psi_{\mathrm{tot}} = \Psi_{\mathrm{el}}\Psi_{\mathrm{vib}}\Psi_{\mathrm{rot}}\Psi_{\mathrm{ns}}. \qquad (5)$$

Bosons with integer values for nuclear spin quantum number I have symmetric Ψ_{tot} [$\Gamma(\Psi_{\mathrm{tot}}) = A_1$], fermions with half integer values of I have antisymmetric Ψ_{tot} [$\Gamma(\Psi_{\mathrm{tot}}) = B_2$]. In general there are $(2I + 1)^2$ possible Ψ_{ns}, of which $(2I + 1)(I + 1)$ are symmetric and $(2I + 1)I$ are antisymmetric. NCCN has two sets of equivalent atoms, but since $I(^{12}\mathrm{C}) = 0$ the carbon atoms have no influence on spin statistics. Since $I(^{14}\mathrm{N}) = 1$ the molecule NCCN is a boson, and the product function Ψ_{tot} has to be symmetric. The electronic ground state $\Psi_{\mathrm{el.}}$ is symmetric. If we consider the ground vibrational state, $\Gamma(\Psi_{\mathrm{vib}}) = A_1$. Thus $\Gamma(\Psi_{\mathrm{rot.}}) = A_1$ must be combined with $\Gamma(\Psi_{\mathrm{ns}}) = A_1$, and $\Gamma(\Psi_{\mathrm{rot}}) = B_2$ with $\Gamma(\Psi_{\mathrm{ns}}) = B_2$. The molecule NCCN exhibits six symmetric and three antisymmetric Ψ_{ns}. Since $\Gamma(\Psi_{\mathrm{rot}}) = A_1$ for even J and $\Gamma(\Psi_{\mathrm{rot}}) = B_2$ for odd J, transitions from states with even J have a statistical weight of six and odd J of three. The first excited bending states $(01)^{1e}$ and $(01)^{1f}$ have B_2 and A_1 symmetry, respectively. Therefore the rotational levels of the $(01)^{1e}$ substate with even J have a statistical weight of three and odd J of six, and vice versa for the $(01)^{1f}$ substate.

SPECTRUM AND ASSIGNMENTS

An overview of the ν_5 band system is given in Fig. 1. The most striking property of the spectrum is the very high line density, due to the small rotational constant B, the

TABLE V

Measured and Assigned Line Positions of the ν_5 Band System of NCCN

J''	P-branch $\tilde{\nu}$/cm^{-1}	(o-c) $\times 10^6$/cm^{-1}	Q-branch $\tilde{\nu}$/cm^{-1}	(o-c) $\times 10^6$/cm^{-1}	R-branch $\tilde{\nu}$/cm^{-1}	(o-c) $\times 10^6$/cm^{-1}
			$(01)^{1e,f} - (00)^{0e}$			
0	–		–		234.036 972*	424
1	(233.407 343)		233.723 631*	812	234.350 719*	-1714
2	233.093 903	-120	233.725 498	78	234.669 095	-78
3	232.781 514	-45	233.729 841	519	234.986 862	97
4	232.469 812	-140	233.734 384	-141	235.305 880*	669
5	232.159 423	220	233.741 256	227	235.623 979*	-530
6	231.849 251	-59	233.749 033	201	235.944 562	-97
7	(231.540 276)		233.757 666	-270	236.265 849	189
8	231.232 629*	529	233.768 346	6	236.587 107*	-404
9	230.924 927	144	233.780 086	43	236.910 142	-71
10	230.618 245	-80	233.793 085	39	237.232 944*	-819
11	230.312 652	-74	233.807 403	55	237.558 007	-156
12	230.008 218	230	233.823 137	188	237.883 588	178
13	229.704 022	-87	233.839 770	-79	238.209 696	192
14	229.401 188	97	233.857 697	-349	238.536 364	-81
15	229.099 196	262	233.877 579	38	238.862 574*	-1657
16	228.796 960*	-678	233.898 436	103	239.192 920	58
17	228.497 101	-103	233.920 334	-88	239.522 395	57
18	228.197 477	-154	233.943 578	-229	239.852 539	-118
19	227.898 688	-232	233.967 351*	-1137	240.183 849	31
20	227.601 016	-55	233.994 022	-442	240.515 765	-57
21	227.303 998	-87	234.021 124*	-610	240.848 733	67
22	227.007 945	-16	234.050 162	-136	241.181 990*	-360
23	226.711 365*	-1335	234.080 068	-88	241.516 848	-26
24	226.418 263	-38	234.111 199	-107	241.852 193	-43
25	226.124 723	-43	234.143 734	-13	242.188 377	-59
26	225.832 008	-86	234.176 808*	-672	242.525 336	-136
27	225.540 205	-81	234.212 269	-234	242.863 379	35
28	225.249 191	-150	234.248 992	177	243.201 980	-70
29	224.958 911*	-348	234.286 682	266	243.541 508	-83
30	224.669 872	-169	234.325 285	-20	243.882 069	105
31	224.381 613	-73	234.366 031*	550	244.223 110	-59
32	224.094 117	-79	234.406 547	-395	244.565 139	-65
33	223.807 490	-79	234.450 182	493	244.908 055	-15
34	223.521 292*	-514	234.493 074*	-645	245.251 690	-74
35	223.236 840	-66	234.539 237	205	245.596 267	-20
36	222.952 856	-15	234.585 435	-193	245.941 594	42
37	222.669 700	1	234.633 528	24	246.287 813	3
38	222.387 247	-143	234.682 596	-63	246.634 768	-41
39	222.105 953	7	234.733 279	185	246.982 349*	-287
40	221.825 339	-26	234.784 725	-80	247.331 238	-38
41	221.545 639	-8	234.837 819	26	247.680 781	39
42	221.266 777	-16	234.892 038	-18	248.030 972	-56
43	220.988 792	-9	234.947 913	320	248.382 156	23
44	220.711 686	13	235.003 165*	-1237	248.734 072	17
45	220.435 295	-113	235.062 634	152	249.086 804	10
46	220.159 993	-13	235.121 792	-39	249.440 367	19
47	219.885 458	-8	235.182 822	373	249.794 683	-34
48	219.611 749	-39	235.244 549	215	250.149 898	0
49	219.338 971	-2	235.305 880*	-1605	250.505 852	-38
50	219.067 002	-18	235.370 359*	-1541	250.862 650	-43
51	218.795 959	31	235.435 033*	-2544	251.220 297	-8
52	218.525 690	-8	235.504 534	19	251.578 774	50
53	218.256 341	12	235.572 659	-53	251.938 048	98
54	217.987 812	-8	235.642 272	104	252.298 002	22
55	217.720 264	91	235.711 339*	-1541	252.658 836	21
56	217.453 314	-71	235.783 448*	-1398	253.020 466	14
57	217.187 471	14	235.856 597*	-1468	253.382 754	-135
58	216.922 411	22	235.931 756*	-779	253.746 259	133
59	216.658 186	6	236.008 205	-50	254.110 060	-102
60	216.394 810	-20	236.085 549	326	254.475 026	32
61	216.132 323	-15	236.160 050*	-3386	254.840 680	59
62	215.870 479	-225	236.243 152	258	255.207 032	-10
63	215.610 616*	688	–		255.574 231	-24
64	215.350 022	13	–		255.942 256	-3
65	215.090 904	-42	–		256.311 070	18
66	214.832 776	36	–		256.680 614	-19
67	214.575 396	7	–		257.050 949	-52
68	214.318 918	24	–		257.422 109	-44
69	214.063 312	59	–		257.794 063	-25
70	213.808 480	14	–		258.166 720	-85
71	213.554 581	48	–		258.540 295	-7
72	213.301 473	21	–		258.914 549	-28
73	213.049 255	30	–		259.289 589	-40
74	212.797 809	-39	–		259.665 053*	-403
75	212.547 413	89	–		260.042 269*	213
76	212.297 705	56	–		260.419 415	-13
77	212.048 816	-9	–		260.797 453	-118
78	211.800 862	12	–		261.176 429	-52
79	211.553 743	20	–		261.556 144	-14
80	211.307 367	-77	–		261.936 520	-81
81	211.062 054	41	–		262.317 598	-208
82	210.817 501	73	–		262.699 767	-6
83	210.573 717	28	–		263.082 332	-167
84	210.330 842	48	–		263.465 937	-46
85	210.088 919	175	–		263.850 089	-134
86	209.847 627	89	–		264.235 142	-76
87	(209.607 174)		–		(264.620 964)	
88	209.367 801	150	–		265.007 387	-74
89	(209.128 970)		–		(265.394 707)	
90	208.891 223	94	–		265.782 831*	131
91	(208.654 127)		–		–	
92	208.418 427*	463	–		–	

J''	P-branch $\tilde{\nu}$/cm^{-1}	(o-c) $\times 10^6$/cm^{-1}	R-branch $\tilde{\nu}$/cm^{-1}	(o-c) $\times 10^6$/cm^{-1}
		$(02)^{2e} - (01)^{1e}$		
1	(233.872 529)		(234.821 499)	
2	(233.558 792)		(235.140 409)	
3	233.245 101*	-1249	(235.460 613)	
4	232.933 540*	-1664	235.783 448*	1336
5	232.624 534*	-821	236.104 897	-9
6	232.317 255	450	236.429 180	182
7	232.009 451	-107	236.753 863	-527
8	231.703 881	266	237.081 291	207
9	231.399 126	147	237.409 241	158
10	231.095 726	72	237.738 465	76
11	230.793 597	-47	238.068 669	-338
12	230.492 169*	-784	238.401 174	234
13	230.193 601	16	238.734 154	-38

Note. Line positions marked with an asterisk were not included in the fit. Line positions in parentheses are calculated.

TABLE V—*Continued*

J''	P-branch $\tilde{\nu}$/cm^{-1}	(o-c) $\times 10^6$/cm^{-1}	R-branch $\tilde{\nu}$/cm^{-1}	(o-c) $\times 10^6$/cm^{-1}
		$(02)^{2e} - (01)^{1e}$		
14	229.895 608	63	239.068 844	76
15	229.598 768	-71	239.404 202	-470
16	229.303 662	191	239.741 859	-51
17	229.009 425	-23	240.080 565	77
18	228.717 108	332	240.420 399	-11
19	228.425 400	-62	240.761 635	-49
20	228.135 442	-70	241.104 336	20
21	227.846 547	-387	241.448 240	-73
22	227.559 778	43	241.793 614	-67
23	227.273 880	-43	242.140 294	-136
24	226.989 509	2	242.488 821	256
25	226.706 469	-26	242.838 189	93
26	226.424 680	-216	243.189 120	90
27	226.144 705	-13	243.541 508	131
28	225.865 969	-3	243.895 102	-43
29	225.588 680	12	244.250 286	-58
30	225.312 822	8	244.606 986	3
31	225.038 321	-100	244.965 045	-25
32	224.764 667*	-833	245.323 678*	-940
33	224.494 051	-11	245.685 578	-56
34	224.224 375	258	246.047 923	-207
35	223.955 467	-208	246.412 080	-36
36	223.688 834	84	246.776 958*	-644
37	223.423 415	64	247.144 860	262
38	223.159 401	-89	247.513 273	157
39	222.897 059	-121	247.883 383	217
40	222.636 571	140	248.254 578	-181
41	222.377 289	34	248.627 912	7
42	222.119 782	118	249.002 557	-58
43	221.863 725	55	249.378 783	-117
44	221.609 491	207	249.757 068	298
45	221.356 496	-22	250.136 138	-98
46	221.105 326	-58	250.517 376	67
47	220.855 734	-160	250.899 924	-73
48	220.608 048	-10	251.284 191	-121
49	220.361 909	21	251.670 235	-27
50	220.117 349	-46	252.057 906	48
51	219.874 599	10	252.446 910	-199
52	219.633 261	-221	252.838 159	136
53	219.394 091	8	253.230 641	31
54	219.156 317	-85	253.624 829	-48
55	218.920 467	17	254.020 521	-311
56	218.686 237	3	254.418 447	-36
57	218.453 985	219	254.817 842	4
58	218.221 561*	-1491	255.218 885	-16
59	217.994 043	-57	255.620 678*	-1003
60	217.766 881	-39	256.026 286	104
61	217.541 509	-9	256.432 413	3
62	–		256.840 937*	567
63	–		257.250 085	20
64	–		257.661 070	-431
65	–		258.074 710	31
66	–		258.489 724	121
67	–		258.906 471	196
68	–		259.324 873	175
69	–		259.744 970	99
70	–		(260.166 797)	
71	–		260.590 529	54
72	–		261.015 429*	-476
73	–		261.442 950	-137

J''	P-branch $\tilde{\nu}$/cm^{-1}	(o-c) $\times 10^6$/cm^{-1}	R-branch $\tilde{\nu}$/cm^{-1}	(o-c) $\times 10^6$/cm^{-1}
		$(02)^{2f} - (01)^{1f}$		
1	(233.872 083)		(234.821 053)	
2	(233.557 455)		(235.139 071)	
3	233.245 101*	1425	235.458 805*	872
4	232.931 461*	716	235.778 274*	632
5	(232.618 665)		(236.098 195)	
6	(232.307 434)		236.419 687	96
7	231.997 530*	476	236.741 903	72
8	231.687 052*	-473	237.064 505*	-409
9	231.379 209*	362	237.388 988	149
10	231.070 935	-87	237.713 771	166
11	230.763 962	-86	238.039 137	-75
12	230.457 653	-274	238.365 616	-42
13	230.151 988*	-670	238.692 875	-68
14	229.848 228	-15	239.021 044	-23
15	229.544 655	-26	239.350 037	9
16	229.241 930	-44	239.679 771	-55
17	228.938 880*	-1240	240.010 326	-134
18	228.639 031	-90	240.341 032*	-896
19	228.339 087	111	240.674 744*	513
20	228.039 601	-85	241.007 117	-250
21	227.741 466	215	241.341 469	134
22	227.443 691	19	241.676 036	-99
23	227.146 850	-98	242.011 742	-24
24	226.851 325	246	242.348 349	124
25	226.555 387*	-679	242.685 598	84
26	226.262 393*	484	243.023 587	-43
27	225.968 451	-157	243.362 459	-114
28	225.676 143	-20	243.702 370	29
29	225.384 575	1	244.042 714	-220
30	225.093 851	9	244.384 398	48
31	224.804 064	99	244.726 704	115
32	224.514 818	-127	245.069 648	-1
33	(224.226 781)		245.412 986*	-544
34	223.938 382*	-1092	245.757 834	-396
35	223.653 164	142	246.103 800	53
36	223.367 788	361	246.450 120	38
37	223.082 118*	-570	246.797 215	-17
38	222.798 809	4	247.144 860	-337
39	222.515 810	32	247.494 129	154
40	222.233 508	-99	247.843 761	195
41	221.952 259	-32	248.193 880	-87
42	221.671 167*	-664	248.545 431	253
43	221.392 197	-30	248.897 220	23
44	221.113 410	-67	249.249 985	-38
45	220.835 536	-47	249.603 521	-134
46	220.558 684	140	249.958 040	-51
47	220.282 297	-62	250.313 352	22
48	220.007 035	7	250.669 661	290
49	219.732 571	20	251.026 166	-47

low-lying term value, and the harmonic nature of the bending mode ν_5. This fact makes it difficult to recognize the positions of the Q branches in the very crowded region between 228 and 235 cm^{-1} (see Fig. 2). Another feature of the spectrum is the

TABLE V—*Continued*

J''	P-branch $\tilde{\nu}$/cm^{-1}	(o-c) ×10^6/cm^{-1}	R-branch $\tilde{\nu}$/cm^{-1}	(o-c) ×10^6/cm^{-1}
		$(02)^{2f} - (01)^{1f}$		
50	219.459 006	77	251.383 601	-252
51	219.186 148	-11	251.742 365	74
52	218.914 192	-51	252.101 563	37
53	218.643 431	251	252.461 434	-120
54	218.372 941	-28	252.822 422	46
55	218.103 605	-5	253.184 161	171
56	217.835 077	-26	253.546 382	-12
57	217.567 302	-145	253.909 853	266
58	217.300 541	-101	254.273 540	-27
59	217.034 647	-41	254.638 377	44
60	216.769 883	299	255.003 884	1
61	216.505 199	-130	255.370 183	-32
62	216.241 915	-8	255.737 324	-5
63	215.979 408	42	256.105 296	75
64	215.717 454	-202	256.473 888	-4
65	215.456 841	46	256.843 282	-56
66	215.196 771	-9	257.213 465	-94
67	214.937 620	9	257.584 742	189
68	214.679 087	-202	257.956 364	47
69	214.422 051	240	258.328 923	72
70	214.165 138	-40	258.702 009	-144
71	213.909 670	281	259.076 393	173
72	213.654 426	-17	259.450 974	-77
73	213.400 269	-70	259.826 649	4
74	213.146 955	-123	260.202 956	-43
75	(212.894 657)		260.579 976	-136
76	212.642 890	-187	260.957 926	-56
77	(212.392 337)		(261.336 606)	
78	212.142 385	-51	261.716 058	74
79	-		(262.096 113)	
80	-		262.477 184	193
81	-		(262.858 616)	
82	-		263.240 902	-86
83	-		263.624 910*	808

J''	P-branch $\tilde{\nu}$/cm^{-1}	(o-c) ×10^6/cm^{-1}	Q-branch $\tilde{\nu}$/cm^{-1}	(o-c) ×10^6/cm^{-1}	R-branch $\tilde{\nu}$/cm^{-1}	(o-c) ×10^6/cm^{-1}
			$(02)^{0e} - (01)^{1e,f}$			
1	230.829 673	-182	231.146 159	422	(231.778 837)	
2	230.516 109	-13	231.147 669	230	232.097 874	119
3	230.203 767	80	231.150 114	122	232.418 408*	442
4	229.891 238*	-1311	231.153 300	-94	232.739 149	-320
5	229.582 643	-65	231.157 740	97	233.062 383	124
6	229.273 529*	-633	231.162 768	31	233.386 243	-91
7	228.967 311*	400	231.168 708	34	(233.711 691)	
8	228.660 745	-206	231.175 474	23	(234.038 326)	
9	228.356 220	-60	231.183 134	69	(234.366 234)	
10	228.052 722	-174	231.191 151	-361	(234.695 410)	
11	227.750 980	185	231.200 783	-5	(235.025 850)	
12	227.450 255	281	231.211 628*	739	(235.357 548)	
13	227.150 449	21	231.221 742	-67	235.689 655*	-843
14	226.851 325*	-829	231.232 629*	-915	(236.024 693)	
15	226.555 387	242	231.245 977	-110	236.360 109	-18
16	226.259 918*	521	231.259 319	-113	236.696 969	176

J''	P-branch $\tilde{\nu}$/cm^{-1}	(o-c) ×10^6/cm^{-1}	Q-branch $\tilde{\nu}$/cm^{-1}	(o-c) ×10^6/cm^{-1}	R-branch $\tilde{\nu}$/cm^{-1}	(o-c) ×10^6/cm^{-1}
			$(02)^{0e} - (01)^{1e,f}$			
17	225.964 920	17	231.273 482	-92	237.034 688	6
18	225.671 727	68	231.288 212	-294	237.373 995	208
19	225.379 705	49	231.304 209	-10	237.713 771	-328
20	225.088 859	-29	231.320 688	-18	238.055 602	-8
21	224.799 294	-54	231.337 176*	-784	238.397 876	-434
22	224.511 107	79	231.355 864	-108	238.741 198*	-991
23	224.224 375	455	231.374 536	-198	239.087 163	-76
24	223.938 382	367	231.394 312	77	239.433 291	-157
25	223.653 164	-140	231.413 489*	-978	239.780 667	-139
26	223.369 813	34	231.435 424	4	240.129 387	86
27	223.087 426	-2	231.457 072	-12	240.478 921	-2
28	222.806 239	-4	231.479 509	61	240.829 661	2
29	222.526 271	58	231.502 254	-248	241.181 990	491
30	222.247 463	135	231.526 166	-68	241.534 482	54
31	221.969 141*	-435	231.550 827	193	241.888 498	62
32	221.692 709	-237	231.575 660	-29	242.243 129	-379
33	221.417 369	-58	231.601 248	-140	242.599 635	2
34	221.143 160	153	231.627 617	-102	242.956 851	55
35	220.869 706	32	231.654 308	-361	243.314 927	-57
36	220.597 406	-9	231.682 115	-112	243.674 268	85
37	220.326 179	-40	231.710 699	321	244.034 723	343
38	220.056 122	50	231.738 561*	-550	244.395 649	88
39	219.786 904	-57	231.768 333	-80	244.757 754	44
40	219.518 720	-155	231.796 927*	-1343	245.120 642	-174
41	219.251 782	-17	231.828 748	79	245.484 866	5
42	218.984 971*	-749	231.859 718	120	245.849 868	34
43	218.720 538	-88	231.891 025	-18	246.215 619	-100
44	218.456 607	104	231.923 042	52	246.582 421	-80
45	218.193 329	-8	231.955 878	450	246.948 394*	-1774
47	217.669 774	-51	232.021 683	-37	247.688 072	-22
48	217.409 350	-103	232.055 532	-16	248.058 271	-55
49	217.149 954	-31	232.089 912	97	248.429 188	-198
50	216.891 475	65	232.124 301	-205	248.801 188	-72
51	216.633 688	-25	232.159 423	-188	249.173 867	-67
52	216.376 980	97	232.195 182	65	249.547 421	26
53	216.120 892	-16	232.231 521	509	249.921 596	-35
54	215.865 759	-15	232.267 407	123	250.296 735	106
55	215.610 616*	-855	232.303 986	64	250.672 374	-2
56	215.357 550	-436	232.341 011	96	251.048 907	47
57	215.105 251	-58	232.379 127*	875	251.426 061	-9
58	214.851 556*	-1872	232.415 633	-291	251.803 950	-44
59	214.602 321	-12	-		252.182 575	-47
60	214.352 024	11	232.491 998	-232	252.561 922	-21
61	214.102 487	28	232.529 264*	-1582	252.941 936	-12
62	213.853 694	33	232.570 078	320	253.322 654	29
63	213.605 565	-45	232.609 501	541	253.704 036	70
64	213.358 234	-64	232.648 679*	237	254.085 840	-123
65	213.111 704	-12	232.688 109*	-89	254.468 556	-51
66	212.865 866	9	232.727 813*	-408	254.851 949	59
67	212.620 842	129	232.767 688*	-815	255.235 760	-44
68	212.376 112	-166	232.808 128*	-912	255.620 678	336
69	212.132 503	-41	232.849 665*	-161	256.005 453	-46
70	211.889 372	-135	232.891 077*	222	256.391 289	22
71	211.647 210	50	232.931 461*	-662	256.777 590	-51
72	211.405 513	15	232.972 749*	-877	257.164 643	28

TABLE V—*Continued*

J''	P-branch $\tilde{\nu}$/cm^{-1}	(o-c) ×10^6/cm^{-1}	Q-branch $\tilde{\nu}$/cm^{-1}	(o-c) ×10^6/cm^{-1}	R-branch $\tilde{\nu}$/cm^{-1}	(o-c) ×10^6/cm^{-1}
			$(02)^{0e} - (01)^{1e,f}$			
73	211.164 450	-66	233.015 124*	-236	257.552 153	-32
74	210.924 215	4	-		257.940 263	-83
75	210.684 602	24	-		258.328 923	-170
76	210.445 805	192	-		258.718 275	-149
77	210.207 240	-74	-		259.108 357	23
78	209.969 695	17	-		259.498 674	-147
79	-		-		259.889 975	94
80	-		-		260.281 519	8
81	-		-		260.673 667	-44
82	-		-		(261.066 478)	
83	-		-		261.459 843	34
84	-		-		261.853 178*	-526
85	-		-		262.248 190	28

J''	P-branch $\tilde{\nu}$/cm^{-1}	(o-c) ×10^6/cm^{-1}	R-branch $\tilde{\nu}$/cm^{-1}	(o-c) ×10^6/cm^{-1}
		$(03)^{3f} - (02)^{2f}$		
2	(234.022 066)		(235.608 991)	
3	(233.707 868)		(235.929 560)	
4	233.394 155*	-578	236.251 165	-24
5	233.083 198*	535	236.573 712	-168
6	232.771 397	-263	236.897 533	98
7	232.462 012	289	237.222 587	143
8	232.153 406	552	237.548 270	-49
9	231.844 970	-85	237.875 008	-248
10	231.538 802	475	238.203 038	-219
11	231.232 629	-44	238.532 242	-79
12	230.927 782	-311	238.862 574	124
13	230.624 218	-371	239.192 920*	-725
14	230.321 588*	-577	239.525 368*	-540
15	230.020 210*	-611	239.858 672*	-567
16	229.719 521*	-1040	240.192 698	-942
17	229.420 503*	-883	240.527 924*	-1189
18	229.123 766	466	240.864 061*	-1598
19	228.826 212	-93	241.203 262	-19
20	228.530 418	14	241.541 956	-25
21	228.235 392	-208	241.881 664	-96
22	227.941 635	-262	242.222 719	97
23	227.648 958	-339	242.564 530	-39
24	227.357 821	16	242.907 540	-64
25	227.067 384	-39	243.251 694	-35
26	226.778 118	-38	243.596 965	18
27	226.489 848	-160	243.943 163	-100
28	226.203 008	25	244.290 742	63
29	225.916 849	-236	244.639 149	-49
30	225.632 042	-277	244.988 777	-49
31	225.348 556	-134	245.338 914	-651
32	225.066 198	-4	245.691 386	-34
33	224.784 838	-23	246.044 308	-87
34	224.504 637	-34	246.398 361	-134
35	224.224 375*	-1264	246.753 710	-15
36	223.947 732	-38	247.110 118	28
37	223.671 063	-7	247.467 623	29
38	223.394 774*	-771	247.826 417	173

J''	P-branch $\tilde{\nu}$/cm^{-1}	(o-c) ×10^6/cm^{-1}	R-branch $\tilde{\nu}$/cm^{-1}	(o-c) ×10^6/cm^{-1}
		$(03)^{3f} - (02)^{2f}$		
39	223.121 148	-54	248.186 025	-19
40	222.848 096	50	248.545 431*	-1571
41	222.575 980	-106	248.909 122	-1
42	222.305 188	-139	249.272 288	-125
43	222.035 726	-51	249.636 937	58
44	221.767 382	-61	250.002 580	51
45	221.500 275	-59	250.369 367	-1
46	221.234 519	62	250.737 344	-61
47	220.969 781	-40	251.106 651	4
48	220.706 391	-43	251.477 127	24
49	220.444 103	-201	251.848 808	29
50	220.183 625	184	252.221 886	200
51	219.923 869	15	252.595 943	112
52	219.665 754	201	252.971 239	16
53	219.408 588	40	253.348 382*	510
54	219.152 716	-132	253.725 954	167
55	218.898 336	-128	254.105 026	47
56	218.643 431*	-1976	254.485 601	144
57	218.393 456	-232	254.867 205	-27
58	218.143 333	16	255.250 368	54
59	217.894 351	44	255.634 874	159
60	217.647 050	381	256.020 175	-270
61	217.400 502	86	256.407 670	153
62	217.156 248*	689	256.795 207*	-734
63	216.912 258	147	257.185 852	121
64	(216.670 086)		257.576 870	-27
65	216.429 316	-179	257.968 042*	-1411
66	216.189 808*	-546	258.363 427	15
67	215.952 725	51	258.758 904	118
68	(215.716 470)		(259.155 588)	
69	215.481 685	-72	259.553 939	106
70	-		(259.953 532)	
71	-		260.354 595	-106
72	-		(260.757 352)	
73	-		261.161 470	-30
74	-		261.565 101*	-2058
75	-		261.973 729*	-614
76	-		262.382 783	-283
		$(03)^{3e} - (02)^{2e}$		
2	(234.022 065)		235.607 696*	-1295
3	(233.707 866)		235.927 701*	-1857
4	233.394 155*	-572	236.251 165	-18
5	233.083 198*	548	236.573 712	-154
6	232.771 397	-235	236.897 533	-71
7	232.462 012	339	237.222 587	192
8	232.153 406*	635	237.548 270	34
9	231.844 970	45	237.875 008	-118
10	231.538 802*	669	238.203 038	-23
11	231.232 629	238	238.532 242	204
12	230.927 782	84	238.862 574*	520
13	230.624 218	167	239.192 920	-185
14	230.321 588	141	239.525 368	182

intensity alternation due to spin statistics. In Fig. 3 the lines of the fundamental band are indicated with an assignment comb. As pointed out in the theoretical section the intensity of lines originating from even J'' should be approximately twice as intense as the adjacent ones with odd J''. An intensity alternation is clearly observable, but a

TABLE V—*Continued*

J''	P-branch $\tilde{\nu}$/cm^{-1}	(o-c) $\times 10^6$/cm^{-1}	R-branch $\tilde{\nu}$/cm^{-1}	(o-c) $\times 10^6$/cm^{-1}
		$(03)^{3e} \leftarrow (02)^{2e}$		
15	230.020 210	328	239.858 672	377
16	229.719 521	168	240.192 698	273
17	229.420 503*	647	240.527 924	351
18	229.121 607	221	240.864 061	328
19	228.824 076	137	241.201 405*	506
20	228.526 883*	-627	241.539 207	140
21	228.231 199*	-896	241.877 465*	-765
22	227.937 614	-74	242.218 333	-48
23	227.644 725	442	242.559 529	14
24	227.351 896	21	242.901 451	-174
25	227.060 392	-66	243.244 706	3
26	226.769 944	-80	243.588 702	-41
27	226.480 574	5	243.933 644	-92
28	226.192 057	-27	244.279 645	-30
29	225.904 425	-138	244.626 512	-40
30	225.617 820	-179	244.974 425	66
31	225.332 362	-21	245.323 678*	592
32	225.047 618	-91	245.672 708	-18
33	224.764 667	698	246.023 277	7
34	224.481 105*	-49	246.374 681	-26
35	224.199 052	-204	246.727 132	102
36	223.918 282	15	247.080 199	-29
37	223.638 338	160	247.434 408	115
38	223.359 119	138	247.789 367	154
39	223.082 118*	1451	248.144 930	-50
40	222.803 325	98	248.501 605	21
41	222.526 271	-381	248.859 079	65
42	222.250 716	-217	249.217 271	11
43	221.976 027	-35	249.576 420	107
44	221.701 926	-104	249.936 117	-45
45	221.428 889	63	250.296 735	-63
46	221.156 539	95	250.658 209*	0
47	220.884 366*	-508	251.020 402*	15
48	220.614 202*	96	251.383 601*	280
49	220.344 216*	82	251.747 147*	145
50	220.074 789*	-158	252.111 578*	158
51	219.806 813*	274	252.476 600*	35
52	219.539 024*	124	252.842 657*	228
53	219.272 024*	0	253.209 431*	430
54	219.006 083*	181	253.576 600*	326
55	218.740 743*	217	253.944 166*	-72
56	218.476 160*	269	254.313 108*	223
57	218.212 549*	560	254.682 587*	379
58	217.949 213*	400	255.050 975*	-1223
59	-		255.423 314*	467
60	-		255.794 520*	371
61	-		256.166 376*	280
62	-		256.539 214*	531
63	-		256.912 596*	693
64	-		257.286 454*	705
65	-		257.661 070*	852
66	-		258.036 009*	706
67	-		258.411 561*	561
68	-		258.788 153*	849
69	-		(259.164 212)	
70	-		259.542 818*	1099
71	-		(259.919 822)	
72	-		260.299 527*	1008

J''	P-branch $\tilde{\nu}$/cm^{-1}	(o-c) $\times 10^6$/cm^{-1}	Q-branch $\tilde{\nu}$/cm^{-1}	(o-c) $\times 10^6$/cm^{-1}	R-branch $\tilde{\nu}$/cm^{-1}	(o-c) $\times 10^6$/cm^{-1}
			$(03)^{1e,f} \leftarrow (02)^{0e}$			
1	231.379 209	-575	231.696 946*	-682	-	
2	231.064 048	-30	231.700 931	270	232.648 679	-133
3	230.747 441*	-1552	231.703 881*	-1330	232.966 560*	-1056
4	230.434 660	128	231.710 699	-580	233.286 926	-113
5	230.121 462*	765	231.719 012	147	233.607 229	149
6	229.807 549	61	231.728 192	221	233.927 950	209
7	229.495 534	626	231.738 561	-36	234.248 992	-30
8	229.182 985	25	231.750 659	-87	234.570 530	-393
9	228.871 746	100	231.764 302	-116	234.892 038*	-1409
10	228.560 990	21	231.779 550	-65	235.215 667*	-927
11	228.250 990	58	231.796 927*	587	235.540 682	316
12	227.941 635	97	231.814 493	-102	235.864 587	-178
13	227.632 557	-234	231.834 255	-127	236.190 164	371
14	227.324 664	-31	231.855 775	72	236.515 420	-32
15	227.017 435	182	231.878 435	-127	236.840 822*	-924
16	226.711 365	895	231.902 954	-6	237.168 776	100
17	226.404 461	111	231.928 280	-622	237.496 472	225
18	226.098 891	-7	231.955 878	-513	237.824 398	-63
19	225.794 174	55	231.985 424	-6	238.153 445	123
20	225.490 144	126	232.016 309	287	238.482 846	13
21	225.186 637	37	232.048 141	-30	238.813 068	68
22	224.883 873	1	232.081 505	-376	239.143 816	-10
23	224.581 856	17	232.116 804	-352	239.475 205	-110
24	224.280 605	98	232.153 406	-594	239.807 376	-97
25	223.979 871	-11	-		240.140 395	90
26	223.680 033	61	232.231 521*	-891	240.473 674	-141
27	223.380 844	62	232.274 386	397	240.808 083	74
28	223.082 118	-202	232.317 255	103	241.142 938	45
29	222.784 533	-60	232.361 824	-81	241.478 499	26
30	222.487 550	-58	232.408 568	315	241.814 734	-20
31	222.191 627	255	232.456 302	101	242.151 427	-317
32	221.895 985	91	232.505 803	49	242.488 821*	-677
33	221.601 234	52	232.556 956	42	242.827 763	-109
34	221.307 181	-61	232.609 501	-187	243.167 062	37
35	221.014 092	8	232.664 044	-35	243.506 961	49
36	220.721 654	-61	232.720 203	112	243.847 559	18
37	220.430 069	-75	232.777 753	24	244.189 158	240
38	220.139 191	-188	232.837 191	194	244.531 067	16
39	219.849 535	106	232.897 904	6	244.873 935	-13
40	219.560 244	-58	232.960 363	-73	245.217 546	-69
41	219.272 024	17	233.024 787	173	245.561 723	-337
42	218.984 971	419	233.090 244	-191	245.907 298	8
43	218.697 947	1	233.158 208	305	246.253 296	-17
44	218.412 159	-38	233.226 490*	-529	246.600 123	-12
45	218.127 279	-35	233.298 225	439	246.948 394*	629
46	217.843 293	-12	233.368 871	-1333	247.296 162	-48
47	217.560 176	-1	233.443 704*	-573	247.645 610	135
48	217.277 949	9	233.519 962	-42	247.995 511	-59
49	216.996 618	16	233.597 601	216	248.346 459	-41

TABLE V—*Continued*

J''	P-branch $\tilde{\nu}$/cm^{-1}	(o-c) $\times 10^6$/cm^{-1}	Q-branch $\tilde{\nu}$/cm^{-1}	(o-c) $\times 10^6$/cm^{-1}	R-branch $\tilde{\nu}$/cm^{-1}	(o-c) $\times 10^6$/cm^{-1}
			$(03)^{1e,f} \leftarrow (02)^{0e}$			
50	216.716 175	6	233.676 905	484	248.698 292	20
51	216.435 681	-968	233.757 666*	556	249.050 926	34
52	216.157 994	-57	233.839 770	318	249.404 372	5
53	215.880 324	-56	233.923 573	129	249.757 068*	-1635
54	215.603 708	64	234.008 677	-407	250.114 169	263
55	215.327 791	-58	234.096 941*	573	250.470 069	89
56	215.053 084	83	-		250.826 911	-21
57	214.779 035	-72	-		251.184 589	-177
58	214.506 178	7	-		251.543 509	22
59	214.234 230	30	-		251.903 062	-37
60	213.963 132	-65	-		252.263 554	-51
61	213.693 088	-80	-		252.625 137	128
62	213.424 259	143	-		252.986 720*	-595
63	213.156 106	61	-		253.350 611	86
64	212.888 956	-3	-		253.714 822	181
65	212.623 209	349	-		254.079 889	223
66	212.357 779	28	-		254.445 745	145
67	212.093 679	45	-		254.812 090	-356
68	211.830 514	4	-		255.180 212	9
69	211.568 256	-126	-		255.548 657	-216
70	211.307 367	118	-		255.918 443	-11
71	211.047 215	102	-		256.288 980	32
72	210.787 965	-8	-		256.660 421	69
73	210.529 754	-76	-		257.032 648	-18
74	210.272 629	-54	-		257.405 781	-108
75	210.016 377	-154	-		257.779 649	-370
76	209.761 323	-50	-		258.155 189	136
77	209.507 290	82	-		258.531 381	392
78	209.254 175	142	-		258.906 471*	-1354
79	209.002 121	274	-		259.285 518	-39
80	208.750 879	232	-		259.665 053*	870
81	208.500 314	-117	-		260.042 269*	-1429
82	208.251 290	94	-		260.422 573*	-1527
83	208.002 880	-59	-		260.805 343	-40
84	207.755 330	-327	-		261.187 785*	240
85	-		-		261.569 903*	-677
86	207.263 765	-239	-		261.954 618	133
87	207.019 108	-517	-		262.338 578*	-676
88	-		-		262.725 229	346
89	-		-		263.110 125*	-1241
90	-		-		263.498 774	74

J''	P-branch $\tilde{\nu}$/cm^{-1}	(o-c) $\times 10^6$/cm^{-1}	R-branch $\tilde{\nu}$/cm^{-1}	(o-c) $\times 10^6$/cm^{-1}
		$(03)^{1f} \leftarrow (02)^{2f}$		
2	(228.022 380)		(229.610 186)	
3	(227.707 036)		(229.929 968)	
4	227.378 166	-14	(230.250 501)	
5	(227.078 590)		(230.571 792)	
6	226.747 321	18	230.863 768	30
7	226.432 844	-20	231.183 134	34
8	226.118 960	-23	231.502 254	38
9	225.805 544	-25	231.820 199	-45
10	225.492 755	-28	232.140 982	49
11	225.180 166	32	(232.516 120)	
12	224.868 008	-36	(232.843 084)	
13	224.556 691	-40	(233.170 933)	
14	224.244 341	45	233.429 534	70
15	(223.984 146)		-	
16	223.625 166	-54	-	
17	223.315 641	-60	-	
18	223.007 040	-66	-	
19	222.699 129	-72	-	
20	222.391 318	80	-	
21	222.085 331	-86	-	
22	221.778 515	-94	-	
23	221.472 742	103	-	
24	221.168 058	112	-	
25	220.864 178	121	-	
26	(220.691 517)		-	
27	220.258 331	-141	-	
28	219.956 441	152	-	
29	219.655 565	164	-	
30	219.355 660	-176	-	
31	219.056 141	-189	-	
32	218.757 915	-202	-	
33	218.459 416	-218	-	
34	218.164 043	-232	-	
35	217.868 111	248	-	
36	217.573 855	-264	-	
37	217.280 574	282	-	
38	216.987 509	-300	-	
39	216.695 980	-320	-	
40	216.405 100	341	-	
41	216.115 789	362	-	
42	215.827 175	385	-	
43	(215.948 117)		-	
44	215.253 686	-433	-	
45	(215.427 772)		-	
46	214.684 150	-487	-	
47	(214.917 116)		-	
48	214.119 071	-547	-	
49	(214.416 676)		-	
50	213.558 602	-612	-	
51	(213.926 980)		-	
52	213.002 188	-684	-	
		$(03)^{1e} \leftarrow (02)^{2e}$		
2	(228.022 097)		229.607 863	-19
3	(227.706 183)		(229.927 108)	
4	(227.390 726)		(230.246 192)	
5	(227.075 728)		230.566 285	101
6	226.764 746	-4	230.885 179	-102
7	226.451 724	5	(231.206 158)	
8	226.140 374	-7	(231.527 054)	
9	(225.820 373)		(231.848 406)	
10	225.518 023	10	(232.170 216)	
11	225.208 122	13	(232.492 484)	
12	224.898 410	-15	(232.815 214)	
13	224.589 195	17	(233.138 407)	
14	224.280 605	19	(233.462 065)	

ratio of 2:1 is never obvious. This is due to the fact that the figure shows a transmittance spectrum, and further due to the distortion of apparent intensity by instrumental factors, which is discussed in the following paper (*15*).

Quantitative data reduction began with the identification and selection of the rovibrational transitions. This is done very efficiently with a Loomis–Wood program

TABLE V—*Continued*

J''	P-branch $\tilde{\nu}$/cm^{-1}	(o-c) $\times 10^6$/cm^{-1}	R-branch $\tilde{\nu}$/cm^{-1}	(o-c) $\times 10^6$/cm^{-1}
		$(03)^{1e} \leftarrow (02)^{2e}$		
15	223 973 056	-21	(233 786 192)	
16	223 666 270	-24	(234 110 790)	
17	223 359 119	-27	(234 435 862)	
18	223 053 145	29	(234 761 410)	
19	222 748 465	33	(235 087 437)	
20	222 442 443	35	(235 413 948)	
21	222 138 011	-37	(235 740 944)	
22	221 834 049	40	236 092 933	-25
23	221 530 668	-43	(236 396 405)	
24	221 227 358	45	236 753 863	-29
25	220 924 973	48	237 083 554	30
26	220 622 861	50	237 416 438	33
27	220 320 920	52	237 748 203	35
28	220 020 041	-55	238 080 999	-37
29	219 719 144	57	238 411 070	360
30	219 418 821	59	238 744 473	-382
31	219 118 792	61	239 079 417	41
32	218 819 209	-62	239 412 802	-42
33	218 520 280	-64	239 747 021	-43
34	218 221 561	65	(240 037 248)	
35	217 922 883	66	240 415 676	44
36	217 624 542	67	240 750 551	-451
37	217 326 837	68	241 085 781	452
38	217 029 254	-68	241 421 015	45
39	216 731 907	-68	(241 712 325)	
40	(216 367 465)		242 092 098	43
41	216 138 126	67	(242 385 751)	
42	215 841 597	66	242 764 338	41
43	215 543 891	63	243 100 634	-40
44	215 248 927	63	243 437 057	38
45	214 953 068	-61	243 773 470	35
46	-		244 110 045	-33
47	-		244 446 211	30
48	-		244 783 742	-27
		$(04)^{4e} \leftarrow (03)^{3e}$		
3	(234 170 554)		236 399 953	339
4	(233 856 329)		236 721 921	-336
5	(233 543 157)		237 045 837	-113
6	(233 231 040)		237 369 888*	-804
7	(232 919 978)		237 696 544	62
8	(232 609 970)		238 023 536	216
9	(232 301 017)		238 351 277	72
10	(231 993 119)		238 680 376	191
11	(231 686 275)		239 010 026	-85
12	(231 380 487)		239 341 288	158
13	(231 075 754)		239 673 151	-42
14	230 771 547*	-529	240 006 397	99
15	230 469 048	-405	(240 340 444)	
16	230 168 035	151	(240 675 630)	
17	229 867 226	-144	241 011 878	23
18	229 568 040	129	241 349 142	24
19	229 269 378	-129	241 687 417	-1
20	(228 972 156)		242 026 915	162
21	228 675 898	38	242 367 131	8
22	228 380 346	-271	242 708 347	-180

J''	P-branch $\tilde{\nu}$/cm^{-1}	(o-c) $\times 10^6$/cm^{-1}	R-branch $\tilde{\nu}$/cm^{-1}	(o-c) $\times 10^6$/cm^{-1}
		$(04)^{4e} \leftarrow (03)^{3e}$		
23	228 086 324	-105	243.050 918	-45
24	227 793 753*	460	243 394 379	-51
25	227 501 193	-19	243 738 581	-346
26	227 210 090	-93	244 084 271	-182
27	226 920 125	-82	244 430 935	-72
28	226.631 221	-64	244 778 411	-176
29	226 343 305	-109	245 127 055	-138
30	226 056 311	-286	245 476 476	-347
31	225 770 571	-261	245 827 277	-200
32	225 485 578*	-542	246 178 748	-406
33	225 201 972*	-488	246 531 410	-442
34	224 919 256*	-596	246 884 988*	-582
35	224 637 742*	-555	247 239 537*	-771
36	224 356 911*	-884	247 595 255*	-811
37	224 077 658*	-688	247 951 794*	-1047
38	223 799 022*	-929	248 309 350*	-1284
39	(223 522 608)		248 668 314*	-1130
40	223 244 426*	-1894	249 029 923*	653
42	222 697 263	355	249 752 155	185
43	222 423 702	-84	(250 114 843)	
44	222 151 527	-193	250 478 651	-81
45	221 880 650	-61	250 843 521	-115
46	(221 610 762)		251 209 658	103
47	221 341 656	-216	(251 576 490)	
48	221 073 637	-406	251 944 535	94
49	220 806 938	-338	252 313 325	-84
50	220 540 510*	-1064	252 683 097	-296
51	(220 276 938)		253 054 375	-21
52	(220 013 369)		253 426 165	-252
53	219 750 521	-348	253 799 787	328
54	219 489 164	-278	254 173 483	-39
55	219 229 047	-42	254 548 434	-174
56	(218 969 813)		254 924 819	100
57	218 711 518	-99	255 301 788	-69
58	-		255 680 157	134
59	-		256 058 913	-307
60	-		(256 439 451)	
61	-		(256 820 718)	
62	-		257 202 360*	-665
63	-		(257 586 374)	
64	-		257 969 517*	-1253
65	-		258 356 106	-110
66	-		(258 742 716)	
67	-		259 130 184	-90
		$(04)^{4f} \leftarrow (03)^{3f}$		
3	(234 170 554)		236.399 953	339
4	(233 856 329)		236.721 921	-336
5	(233 543 157)		237 045 837	-113
6	(233 231 040)		237 369 888*	-804
7	(232 919 978)		237 696 544	62
8	(232 609 970)		238 023 536	216
9	(232 301 016)		238 351 277	73
10	(231 993 118)		238 680 326	191
11	(231 686 274)		239 010 026	-84

TABLE V—*Continued*

J''	P-branch $\tilde{\nu}$/cm^{-1}	(o-c) $\times 10^6$/cm^{-1}	R-branch $\tilde{\nu}$/cm^{-1}	(o-c) $\times 10^6$/cm^{-1}
		$(04)^{4f} \leftarrow (03)^{3f}$		
12	(231 380 486)		239 341 288	160
13	231 075 925	174	239.673 151	-39
14	230 771 547*	-525	240.006 397	103
15	230 469 048	-398	240 341 032*	595
16	230 168 035	160	240 674 744*	-877
17	229 867 226	-131	241 011 878	36
18	229 568 040	147	241 349 142	43
19	229 269 378	-103	241 687 417	25
20	228 971 834	-288	242 026 915	196
21	228.675 898	84	242 367 131	53
22	228 380 346	-211	242 708 347	-120
23	228 086 324	-27	243 050 918	34
24	227 793 753*	560	243 394 379	50
25	227 501 193	109	243 738 581	-218
26	227 210 090	68	244 084 271	-20
27	226 920 125	119	244 430 935	131
28	226 631 221	186	244.778 411	76
29	226 343 305	198	245 127 055	172
30	226 056 311	90	245 476 476	31
31	225 770 571	195	245.827 277	260
32	225 485 578	9	246 178 748	150
33	225 201 972	174	246 531 410	226
34	224 919 256	193	246 884 988	215
35	224.637 742	382	247.239 537	176
36	224 356 911	224	247.595 255	309
37	224 077 658*	616	247 951 794	272
38	223 799 022*	600	248 309 350	261
39	223 521 292*	468	248 668 314*	674
40	223 244 426	180	249.027 346	174
41	222 969 106*	422	249 387 666	-16
42	222 694 418	283	249 749 386	221
43	222 420 594	-2	(250 111 616)	
44	222 148 141	79	250 475 014	-16
45	221 876 533	2	250 839 483	80
46	221 605 547*	-450	251 204 754	24
47	221 336 030*	-426	251 570 885	-120
48	221 067 822	-82	251 938 048	-174
49	220 800 130	-206	252 306 489	114
50	220 533 827	80	252.675 381	-79
51	220 268 000	-132	253 045 544	76
52	220 004 300*	815	253 416 444	50
53	219 739 854	55	253 788 442	212
54	219 477 058	-13	254 161 121	151
55	-		254 534 779	173
56	-		254.909 123	-7
57	-		255.284 123	-411
58	-		255 660 832	21
59	-		256 037 692	-259
60	-		256 416 277	331
61	-		256 795 207	421
62	-		257 174 698	236
63	-		257.555 036	72
64	-		257 936 241	-42

J''	P-branch $\tilde{\nu}$/cm^{-1}	(o-c) $\times 10^6$/cm^{-1}	Q-branch $\tilde{\nu}$/cm^{-1}	(o-c) $\times 10^6$/cm^{-1}	R-branch $\tilde{\nu}$/cm^{-1}	(o-c) $\times 10^6$/cm^{-1}
			$(04)^{0e} \leftarrow (03)^{1e,f}$			
1	228 971 834*	934	-		(229 926 284)	
2	228 656 565*	1098	229.289 793	93	(230 247 767)	
3	228.341 756	206	-		(230.570 757)	
4	228.028 612*	-533	229.294 693*	682	(230.895 246)	
5	227 718 446	195	229 296 839	-240	(231.221 230)	
6	227 408 954	91	229 299 990*	-759	(231.548 700)	
7	227 100 701	-276	229 303 662*	-1352	(231 877 648)	
8	226 794 341	-246	229 309 992	126	(232 208 065)	
9	226 489 848	162	229.315 251	-46	(232.539 939)	
10	226.186 515	250	229.321 305	7	(232.873 259)	
11	225.884 371	55	229 326 704*	-1152	(233.208 012)	
12	225.584 036	209	229 335 068	106	(233.544 184)	
13	225 284 701	-86	229 342 534	-66	(233.881 759)	
14	224 987 259	76	229 350 645	-114	(234 220 722)	
15	224 691 215	213	229 359 417	-4	(234 561 054)	
16	224 394 855*	-1375	229 368 556	-17	(234 902 739)	
17	224 102 964	115	229 377 894	-302	(235 245 756)	
18	223.810 781	-62	229.388 350	76	(235.590 085)	
19	223 521 292*	1098	229 401 188*	2402	(235.935 705)	
20	223 230 906	23	229 409 963	249	236.282 599	5
21	222 942 895	5	-		236.630 058*	-670
22	222 656 111	-84	-		236 980 100	16
23	222 370 755	-20	-		237.330 483	-153
24	222 086 608	0	-		237 682 641	281
25	221.803 688	17	-		238 034 554*	-676
26	221.521 925	-14	-		238.389 137	-80
27	221.241 438	51	-		238.744 473	177
28	220 961 958	-33	-		239.100 567	128
29	220 683 710	-14	-		239 457 690	73
30	220 406 737	178	-		239 815 950	148
31	220.130 428	-42	-		240 175 004	39
32	219.855 431	0	-		240 534 649	-430
33	219.581 302	-111	-		240.896 246	131
34	219.308 455	66	-		241 258 110	67
35	219.036 335	3	-		241.620 906	69
36	218 765 180	-35	-		241 984 928	460
37	218 495 022	11	-		242.351 571*	2661
38	218.225 828	134	-		242.713 937	-198
39	217.957 199	-39	-		243.080 245	127
40	217.689 740	124	-		243.446 956	123
41	217.422 987	182	-		243.814 057	-200
42	217.156 248*	-532	-		244 182 528	163
43	216 891 475	-43	-		244.551 039	-98
44	216.627 000	2	-		244.920 999	449
45	216.363 081	-117	-		245.290 528	-56
46	216.100 057	-40	-		245.661 516	294
47	215.837 568	-110	-		246.032 353	-93
48	215.575 693	-230	-		246.404 043	-196
49	215.314 748	-67	-		246 776 958	371
50	215.053 084*	-1255	-		247 149 080	-396
51	214 794 330	-152	-		-	
52	214 535 062	-170	-		-	
53	214 276 189	-387	-		-	
54	214 018 205	-302	-		-	
55	213.760 820	-194	-		-	
56	213.503 690	-401	-		-	
57	213.247 520	-213	-		-	

for the *P* and *R* branches (*19*) and with the program QBRASS for the *Q* branches (*20*). These programs use the calibrated peak list and allow the selection of the individual rovibrational lines into subbands based on the power series representation of Eq. (1). The lines of each subband are written separately on a file. The vibrational

TABLE V-*Continued*

J''	P-branch $\tilde{\nu}$/cm^{-1}	(o-c) ×10^6/cm^{-1}	R-branch $\tilde{\nu}$/cm^{-1}	(o-c) ×10^6/cm^{-1}
		$(04)^{2e} \leftarrow (03)^{1e}$		
6	230.361 518*	-2009	-	
7	230.054 969	-719	-	
8	229.749 778	389	-	
9	229.444 546	-91	-	
10	229.140 708*	-736	-	
11	228.838 715*	-1106	236.164 036*	-527
12	228.539 635	-146	236.501 723	217
13	228.241 516	179	-	
14	227.944 140	-366	237.180 065	-170
15	227.648 958	-344	237.521 998	-56
16	227.354 757*	-986	237.865 432	-100
17	227.063 542	-306	238.209 696*	-994
18	226.773 187	-449	238.557 758	211
19	226.485 707*	579	238.905 853	-273
20	226.197 157*	-1188	239.256 719	272
21	225.913 415	104	239.608 563	29
22	225.628 725*	-1323	239.962 298	-113
23	225.348 556	-25	240.318 036	-68
24	225.069 031	95	240.674 744*	-892
25	224.791 169	31	241.034 866	-170
26	224.514 818	-397	241.396 325	-3
27	224.239 471*	-1722	241.759 834	292
28	223.967 657*	-1445	242.124 623	-80
29	223.699 478*	509	242.491 844	3
30	223.430 784	-40	-	
31	223.164 582	-113	243.231 973	-187
32	-		243.605 371	-25
33	222.638 610	3	243.980 956	234
34	222.377 289*	-1417	244.357 736	-430
35	222.119 782*	-1158	244.737 691	-63
36	221.863 725*	-1613	245.120 642*	1128
37	-		245.503 181	-291
38	-		245.889 141	-513
39	-		246.277 654	-432
40	-		246.668 106*	-684
41	-		247.061 193	-597
42	-		247.456 505	-602
43	-		247.854 533	-229
44	-		248.254 578	-197
45	-		248.656 259*	-903
		$(04)^{2f} \leftarrow (03)^{1f}$		
15	227.539 097	-475	-	
16	227.230 934	-71	-	
17	226.923 058	-6	-	
18	226.615 853	105	238.397 876*	805
19	226.309 106	46	238.727 259	230
20	226.002 924	-76	239.057 785	198
21	225.697 684	115	239.388 808	64
22	225.393 160	392	239.720 556	57
23	225.088 859	260	240.051 831*	-1022
24	224.784 838	-225	240.386 152	347
25	224.481 105*	-1055	240.719 432	77
26	224.179 776	-117	241.053 513	10
27	223.878 317	55	241.388 217	-31
28	223.577 244	-25	241.723 624	33
29	223.276 883	-32	242.059 323	-208
30	222.977 205	2	242.396 217	148
31	222.678 265	132	242.733 497	292
32	-		243.071 068	129
33	-		243.409 162	-110
34	221.784 815	19	243.748 120	-83
35	221.488 364	49	244.088 356*	621
36	221.192 350	-136	244.428 489*	623
37	220.897 382	71	244.768 895	296
38	220.602 824	31	245.109 970	37
39	220.309 660*	726	245.451 504	-367
40	220.015 921	184	245.794 692	280
41	219.723 247	42	246.137 764	205
42	219.431 620	280	246.481 226	-87
43	219.140 365	219	246.825 859	183
44	218.849 829	204	247.170 596	-53
45	218.559 926	145	-	
46	218.270 533	-85	247.862 929*	495
47	217.982 185	46	248.209 393	142
48	217.694 634	286	248.556 804	117
49	-		248.904 915	171
50	217.120 996	148	249.253 342	-85
51	216.834 239*	-907	249.603 521*	784
52	216.550 302	151	249.952 705	26
53	216.266 097	231	250.303 662	406
54	215.982 401	104	250.654 630	159
55	215.699 134	-315	251.005 817*	-511
56	215.417 433	106	251.358 891	58
57	215.136 074	136	251.711 391*	-597
58	-		252.065 808	8
59	214.575 396	16	252.420 909*	637
60	214.296 357	132	252.775 524	113
61	214.018 205	378	253.131 533	313
62	213.740 248	53	253.487 877	170
63	213.463 335	1	253.844 897	19
64	213.187 245	-8	254.202 750	13
65	212.910 561*	-1398	254.560 232*	-1060
66	212.636 159*	-1300	254.920 426	-123
67	212.363 786	23	-	
68	212.090 573	-306	255.641 477	279
69	211.818 147*	-667	256.001 521*	-1083
70	-		256.364 800	59
71	-		256.727 371	-246
72	-		257.091 309	69
73	-		-	
74	-		257.820 798	41
75	-		258.185 491*	-1178
76	-		258.553 382	22
77	-		258.921 220*	380
78	-		259.289 589*	472
79	-		259.658 112	-87

assignment and the J assignment are confirmed or if necessary corrected by the use of the combination differences.

The assignment was almost straightforward since the ground state constants and those of the ν_5 manifold $(0n)$ states with n up to 2 were already known sufficiently well from the literature (*4, 5, 6, 7, 22*). Transitions with v_5 up to 4 were finally assigned. In Fig. 2 the band origins of each subband are indicated.

From the hot band $(11) \leftarrow (10)$ in the ν_5 band system only two of the four subbands could be identified, since only information about the $(10)^{1e}$ substate is available in the literature (*4*) and the spectrum is too dense to allow assignment of the subbands originating from the $(10)^{1f}$ substate without auxiliary information. Therefore the combination band system $\nu_4 + \nu_5$ will be measured at high resolution to fix the upper states of the missing subbands. Also the ν_5 fundamental of the isotopomer $N^{13}CCN$, which should in principle be detectable with its $\approx 2\%$ natural abundance, could not be assigned unambiguously. An extended investigation of all band systems needed to characterize all the singly excited vibrational states, and the combination state of the two bending modes (11), is in progress. The measurement for the parent cyanogen and various isotopomers are partially completed and will be the topic of a subsequent publication.

MOLECULAR CONSTANTS OF CYANOGEN IN THE ν_5 MANIFOLD

Over 1500 rovibrational lines were collected into 16 different subbands. First, each subband was fitted separately to Eq. (1), yielding the power series molecular constants. The band centers of each subband are given in Table II. Table III contains the power series rotational constants of each sublevel and indicates from which transition the

TABLE VI

Comparison of Experimental Vibrational and Rotational Constants of the ν_5 Band System of NCCN with ab Initio Results (the Numbers in Parentheses Give One Standard Deviation in Units of the Last Digits Given)

Parameter	This work	*Ab initio*	Ref.	Experimental	Ref.
ω_5	234.2530 (50)[b]	249.0	(*23*)	234.4	(*24*)
x_{55}	-0.4697 (70)			-0.4	(*24*)
$x_{k,e}$	0.9508 (11)[a]				
$x_{k,5}^{(v)}$	0.01068 (28)				
B_0	0.15708769 (14)			0.157073 (5)	(*22*)
				0.157115 (20)	(*5*)
				0.157135 (10)	(*4*)
				0.157124 (7)	(*6*)
B_e	0.15654618 (96)[a]	0.154 43	(*23*)		
$10^4\alpha_5$	5.4291 (73)[b]	4.830	(*13*)	5.45 (3)	(*5*)
				-5.48 (5)	(*6*)
$10^6\gamma_{55}$	1.20 (12)			-4.5 (15)	(*6*)
$10^8 D_0$	2.1106 (16)			2.7 (5)	(*5*)
				2.50 (8)	(*4*)
				2.63 (8)	(*6*)
$10^8 D_e$	2.0211 (67)[a]	2.008	(*23*)		
		2.003	(*25*)		
$10^{10}\beta_{55}$	9.22 (20)				
$10^{15} H_e$		1.3	(*25*)		
$10^4 q_5$	2.22824 (23)			3.19	(*4*)
				2.259 (9)	(*6*)
$10^4 q_{5,e}$	2.2154 (15)[a]	2.051	(*13*)		
$10^7 q_5^{(v)}$	6.20 (42)				
$10^{10} q_{5,J}$	6.114 (80)	4.67	(*21*)		

[a] The estimated contributions of the linear terms (Y_i) in $v_i (i \le 4)$ are larger than the error of this constant (X^*):

$$X^* = X + \sum_{i=1}^{4} Y_i \frac{d_i}{2}.$$

[b] The estimated contributions of the higher order terms (Z_{i5}) in v_i and $v_j (i \le 4)$ are larger than the error of this constant Y_5^*:

$$Y_5^* = Y_5 + \sum_{i=1}^{4} Z_{i5} \frac{d_i}{2}.$$

constants were derived. At this stage of data reduction the quality of the lines was checked. Overlapped lines were omitted if the differences between observed and calculated transition wavenumber (obs-calc) exceeded 1×10^{-3} cm^{-1}.

The constants given in Tables II and III, also valuable for quick calculations, are used to determine estimates of the constants of the effective Hamiltonian [Eqs. (2–4)], as starting values for fitting these constants to the observed transitions. The program presently allows simultaneous fitting of four states. All lines left in the fit were weighted equally. The transitions were split into two fits. The first contained all transitions within four states up to $v_5 = 3$. The second fit contained the states (03) and (04) where the constants of the (03) state were taken from the first fit and held fixed. The resulting constants are given in Table IV. Over 1500 transitions are represented by only 32 spectroscopic constants. In Table V all lines of every subband are given together with the (obs-calc)-values from the effective Hamiltonian fit.

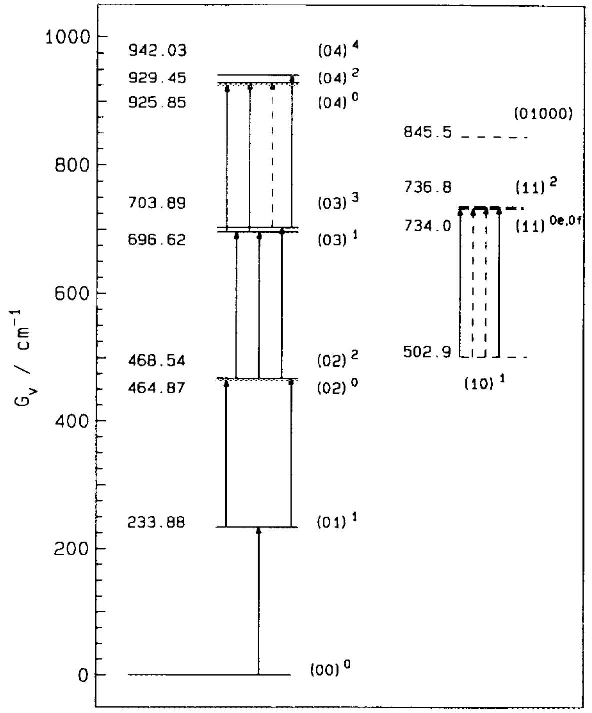

FIG. 4. Vibrational term (G_v) diagram of NCCN. The assigned transitions are indicated with solid arrows. Dashed states are taken from the literature (*4*). Transitions marked with dashed arrows should be detectable in the spectrum, but could not be assigned.

DISCUSSION

Cyanogen is among the few molecules in which rovibrational transitions may be observed up to a vibrational quantum number of four, without any observable resonance interactions with other normal modes. Therefore it is easy to check the convergence of the expansion of the molecular constants in the vibrational quantum numbers:

$$G_{v_1,\ldots,v_5} = \sum_i \omega_i\left(v_i + \frac{d_i}{2}\right) + \sum_i \sum_{j\geq i} x_{ij}\left(v_i + \frac{d_i}{2}\right)\left(v_j + \frac{d_j}{2}\right),$$

$$B_{v_1,\ldots,v_5} = B_e - \sum_i \alpha_i\left(v_i + \frac{d_i}{2}\right) + \sum_i \sum_{j\geq i} \gamma_{ij}\left(v_i + \frac{d_i}{2}\right)\left(v_j + \frac{d_j}{2}\right),$$

$$D_{v_1,\ldots,v_5} = D_e + \sum_i \beta_i\left(v_i + \frac{d_i}{2}\right),$$

$$q_{v_1,\ldots,v_5} = q_e + \sum_i q_i^{(v)}\left(v_i + \frac{d_i}{2}\right).$$

$$x_{k,v_1,\ldots,v_5} = x_{k,e} + \sum_i x_{i,k}^{(v)}\left(v_i + \frac{d_i}{2}\right). \quad (6)$$

The resulting coefficients are given in Table VI in comparison with experimental and ab initio values in the literature.

The results of ab initio calculations may help to find unassigned experimental transitions. On the other hand the comparison between experimental and calculated values is a touchstone for the theoretical and/or numerical basis of the calculations for species less accessible experimentally. If the difficulties in calculating effects on the order of several Hz for q_{5J} are considered, the comparison between the experimental and calculated values (see Table VI) is remarkable.

The derived molecular constants help us to understand the structure of the ν_5 fundamental band system. The relatively small rotational constant and rotation–vibration interaction constant lead to a high density of lines within one subband. Furthermore a significant population of rotational levels is achieved for J up to ≈ 90. The small values for the anharmonicity constant x_{55} and the k-dependent part of the vibrational energy causes the origins of each subband within the ν_5 band system to lie very close to the fundamental origin. The origins of all assigned subbands are extended only over a region of ≈ 7 cm^{-1}. The very high line density makes it difficult to assign transitions of NCCN from "dark" infrared states, and from other isotopomers, for which the spectroscopic constants are not sufficiently well known.

The vibrational term diagram is given in Fig. 4. It shows graphically that NCCN is a rather rigid linear molecule. The term values of the k substates within each state increase with increasing k.

ACKNOWLEDGMENTS

Klaus Lattner is thanked for his assistance in recording the Fourier-transform spectra of C_2N_2. Fred Stroh is thanked for making available the programs LW51, QBRASS4, and FITEFF. This work was supported by funds from the Deutsche Forschungsgemeinschaft and the Fonds der Chemischen Industrie.

RECEIVED: December 22, 1992

REFERENCES

1. L. J. GAY-LUSSAC, *Ann. Chim.* **95,** 172–199 (1815).
2. P. BRUN AND A. FONTAINE, *Noveau traité de chimie minérale, VIII, Carbon, Masson et C^ie Éditeurs, Paris, first edition* 1968.
3. T. K. BROTHERTON AND J. W. LYNN, *Chem. Rev.* **59,** 841–883 (1959).
4. I.-Y. WANG AND A. WEBER, *J. Chem. Phys.* **67,** 3084–3096 (1977).
5. A. PICARD, *Spectrochim. Acta Part A* **30,** 691–701 (1974).
6. K. JOLMA, *J. Mol. Spectrosc.* **92,** 33–39 (1982).
7. H. G. M. EDWARDS AND H. R. MANSOUR, *J. Mol. Struct.* **160,** 209–219 (1987).
8. V. G. KUNDE, A. C. AIKIN, R. A. HANEL, D. E. JENNINGS, W. C. MAGUIRE, AND R. E. SAMUELSON, *Nature* **292,** 686–688 (1981).
9. A. COUSTENIS, B. BÉZARD, AND D. GAUTIER, *Icarus* **80,** 54–76 (1989).
10. F. STROH AND M. WINNEWISSER, *Chem. Phys. Lett.* **155,** 221–226 (1989).
11. F. STROH, Ph.D. Thesis, Justus-Liebig-Universität Giessen, 1991.
12. P. BOTSCHWINA, *Chem. Phys.* **81,** 73–85 (1983).
13. P. BOTSCHWINA AND J. FLÜGGE, *Chem. Phys. Lett.* **180,** 589–593 (1991).
14. H. RUBENS AND H. V. WARTENBERG, *Physik. Zeitschr.* **XII,** 1080–1084 (1911).
15. J. C. GRECU, B. P. WINNEWISSER, AND M. WINNEWISSER, *J. Mol. Spectrosc.* **159,** 551–571 (1993).
16. G. M. PLUMMER, G. WINNEWISSER, M. WINNEWISSER, J. HAHN, AND K. REINARTZ, *J. Mol. Spectrosc.* **126,** 255–269 (1987).
17. M. BIRK, M. WINNEWISSER, AND E. A. COHEN, *J. Mol. Spectrosc.* **136,** 402–445 (1989).

18. K. M. T. YAMADA, F. W. BIRSS, AND M. R. ALIEV, *J. Mol. Spectrosc.* **112,** 347–356 (1985).

19. B. P. WINNEWISSER, J. REINSTÄDTLER, K. M. T. YAMADA, AND J. BEHREND, *J. Mol. Spectrosc.* **136,** 12–16 (1989).

20. F. STROH, Documentation for the program QBRASS, Justus-Liebig-Universität Giessen, 1991 (unpublished).

21. P. BOTSCHWINA, private communication (1991).

22. A. G. MAKI, *J. Chem. Phys.* **43,** 3193–3199 (1965).

23. P. BOTSCHWINA AND P. SEEBALD, *Chem. Phys.* **141,** 311–323 (1989).

24. L. H. JONES, *J. Mol. Spectrosc.* **49,** 82–90 (1974).

25. P. BOTSCHWINA, *J. Mol. Struct.* **88,** 371–381 (1982).